

Review

Hydraulic Jump: A Brief History and Research Challenges

Diana De Padova *  and Michele Mossa 

Department of Civil, Environmental, Land, Building Engineering and Chemistry (DICATECh),
Polytechnic University of Bari, Via E. Orabona 4, 70125 Bari, Italy; michele.mossa@poliba.it

* Correspondence: diana.depadova@poliba.it

Abstract: This paper presents a brief history of the hydraulic jump and a literature review on hydraulic jumps' experimental and numerical studies. Leonardo da Vinci noticed this phenomenon early on, but it was only later studied by Bidone in 1820. Since the beginning of the 20th century, the hydraulic jump has received a lot of attention following the development of energy dissipater designs and stilling basins. The late 1920s and early 1930s saw many experimental studies researching the surface roller profile and energy dissipation. The study of internal flow features started in the late 1950s. Starting in the 70s, it was believed that the flow of a jump must be analyzed in its actual configuration of air–water mixture, an aspect that cannot be overlooked. Several experimental studies in the late 1980s and 1990s highlighted the existence of oscillating phenomena under specific flow conditions and particularly, a cyclic variation of jump types over long-lasting experiments. The early 2000s saw many experimental studies researching the complex structure of the separated region in very large channels downstream of the lateral shockwaves. Whereas most of the experiments provide measurements at a point or on a plane, the complete flow field supplied by CFD simulations enables us to have a deeper understanding of the dynamics of coherent structures that are responsible for free-surface fluctuations and aeration in hydraulic jumps. Therefore, in recent years, the computational fluid dynamics (CFD) method, through turbulence models, has become a useful tool to study this complex environmental fluid mechanic problem.



Citation: De Padova, D.; Mossa, M. Hydraulic Jump: A Brief History and Research Challenges. *Water* **2021**, *13*, 1733. <https://doi.org/10.3390/w13131733>

Academic Editor: António Pinheiro

Received: 6 May 2021

Accepted: 17 June 2021

Published: 23 June 2021

Publisher's Note: MDPI stays neutral with regard to jurisdictional claims in published maps and institutional affiliations.



Copyright: © 2021 by the authors. Licensee MDPI, Basel, Switzerland. This article is an open access article distributed under the terms and conditions of the Creative Commons Attribution (CC BY) license (<https://creativecommons.org/licenses/by/4.0/>).

Keywords: hydraulic jumps; oscillating characteristics; vorticity; pressure; smoothed particle hydrodynamics modelling

1. Introduction

The jump of Bidone or hydraulic jump was described by Bidone [1] with the following words: “If, when a stream has been established in a rectangular channel . . . the flow of water is totally impeded by lowering a gate in any section of the channel itself, the waters thus restrained rise immediately up to a certain height against the gate and form an intumescence”. As an example, Figure 1 shows some pictures of a hydraulic jump in the channel of the LIC—Coastal Engineering Laboratory of the Polytechnic University of Bari, Italy, characterized by a large aspect ratio, since it is 15 m long, 4 m large and 0.4 m high.

Although Bidone [1] was the first to experimentally and analytically analyze the hydraulic jump experimentally and analytically, Leonardo da Vinci noticed this phenomenon earlier. In fact, he sketched the streamline distribution in a vortex and the formation of eddies at an abrupt expansion (Figure 2), which a hydraulic jump resembles.

In 1939, Guglielmini [2] sketched a hydraulic jump in plate 9 (Figure 3) in the book “DALLA NATURA DE’ FIUMI”, using the following comments: “Let us assume . . . that the water, running out of B and entering channel BG, less inclined but wider, requires to discharge a height BI less than CH: in such a case, it is observed that the water descending through AB does not take its surface CD to join that of DE, but it sinks, as in ED, below level EF; and the water in ED is left hanging, so that the stream surface is maintained at CDEF.”



Figure 1. A hydraulic jump in the large channel of the LIC—Coastal Engineering Laboratory of the Polytechnic University of Bari, Italy. (See Video S1 in Supplementary Material).

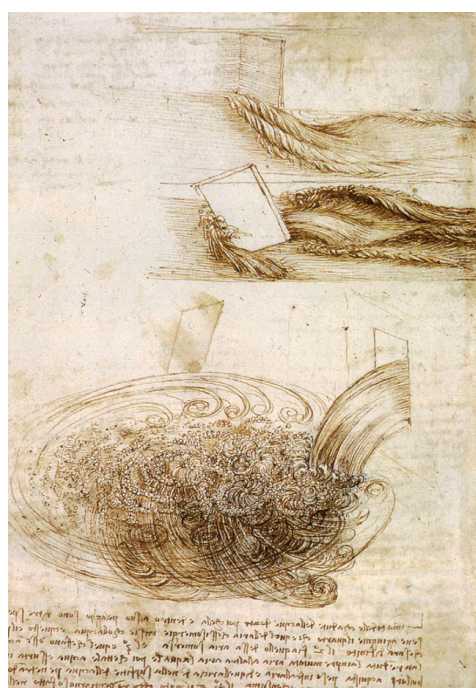


Figure 2. A free water jet issuing from a square hole into a pool.

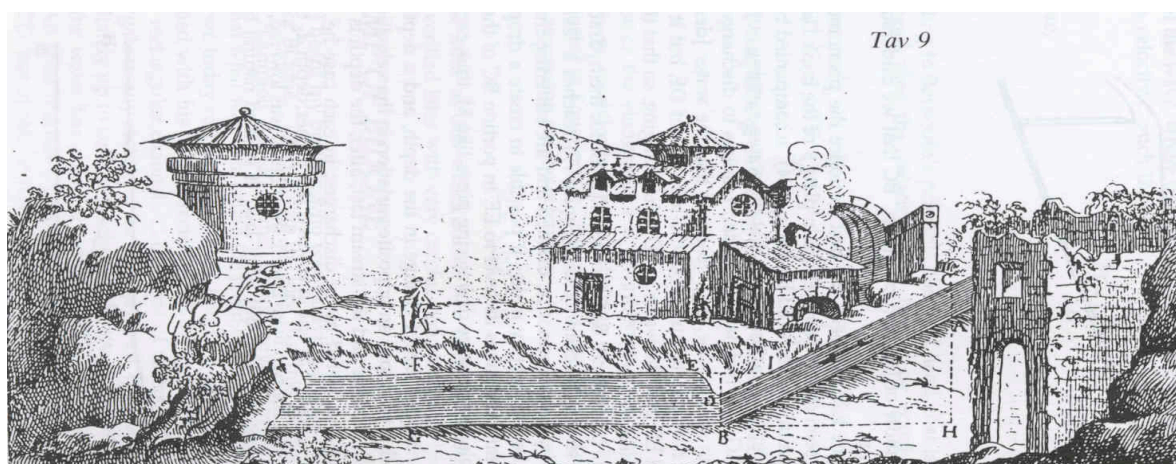


Figure 3. Hydraulic jump (by Guglielmini [2]).

The hydraulic jump occurs whenever an upstream supercritical flow is forced to become subcritical. Bidone tested many discharges and understood that the lower upstream depth d_1 was linked to the higher downstream depth d_2 with the following equation:

$$d_2 - d_1 = \frac{V_1^2 - V_2^2}{2g} \quad (1)$$

where g is the gravitational acceleration, and V_1 and V_2 are the upstream and down-stream velocity, respectively.

About ten years later, Jean Baptiste Bélanger [3] noted that Bidone's experimental results did not agree with Equation (1); therefore, starting from the momentum conservation principle, he discovered the now famous Bélanger equation for undeveloped inflow (see [4]), which considers the head loss of the flow:

$$\frac{d_2}{d_1} = \frac{1}{2} \left(\sqrt{1 + 8Fr_1^2} - 1 \right) \quad (2)$$

where Fr_1 is the inflow Froude number ($Fr_1 = V_1 / \sqrt{gd_1}$).

Harleman [5] found discrepancies with respect to Equation (2); in particular, for high inflow Froude numbers, Harleman [5] showed that the sequent depth-ratio values were lower.

2. State of the Art

The classic hydraulic jump has been widely studied by Peterka [6], Rajaratnam [7], Leutheusser and Kartha [8], Hager and Bretz [9], Hager and Bremen [10], Hager [11], Wu and Rajaratnam [12] and CarolloFerro [13].

Since the beginning of the 20th century, the hydraulic jump has received a lot of attention with the development of energy dissipater designs and stilling basins [14,15].

It is well known that one of the objectives of the designer is to ensure that the jump will not be swept out of the basin, and the design process would involve the determination of optimum basin floor elevation, required tailwater elevation, adequate basin length and desired blocks and end sills. A review of different types of basins can be found in Hager [15].

Riegel and Beebe [16] did experiments on the performance of stilling basins with different sloping bottoms, expansion angles and dimension blocks. The dentated sill was introduced by Rehbock [17].

2.1. Experimental Studies on the Internal Flow in Hydraulic Jumps

In the late 1920s and early 1930s, several experimental studies looked into the surface roller profile and energy dissipation. Safranez [18] credited the energy loss to the rotational movement in the roller. Bakhmeteff [19] focused on open channel flows and defined the concept of specific energy. Rouse [20] emphasized the Froude number Fr as an important parameter useful to characterize a hydraulic jump.

In 1932–1933, the Fluid Mechanics Laboratory of Columbia University, in New York, N.Y., USA, focused its research on the longitudinal elements of the jump using the principle of dynamic similarity, and the final data were presented in generalized dimensionless form. While the dimensionless presentation in terms of dynamic similarity was a matter of course when it came to flow in closed conduits, its application to open flow was not yet widespread. Bakhmeteff and Matzke [21] showed general dimensionless characteristics of the jump in terms of ‘the kinetic flow’ λ :

$$\lambda = 2 \frac{\varepsilon_k}{\varepsilon_p} = \frac{V^2}{gd} = \frac{q^2}{gd^3} \quad (3)$$

which is expressed by twice the ratio of the kinetic energy head (ε_k) to the potential energy head (ε_p) contained in each unit of weight of liquid, flowing at depth d , velocity V and unit discharge q . In the terms ordinarily used in studies of dynamic similarity, the kinetic flow factor λ is equivalent to the so-called Froude number.

The late 1950s saw the start of the studies into internal flow features; the first turbulence estimations in hydraulic jumps were studied by Rouse et al. [22]. In their study, the air interface of a typical hydraulic jump profile was replaced by a solid wall, and air was used in their model. Through the analysis of turbulence measurements conducted in the air-flow model of the hydraulic jump under conditions simulating three representative Froude numbers, Rouse et al. [22] obtained important information on the energy transformation. Rouse et al. [22] could be included in the group of papers where an analogy of the hydraulic jump with other flows is used.

On this topic, the study by Rajaratnam [7] was particularly interesting. In particular, Rajaratnam [6] studied the hydraulic jump, treating it as an example of a plane turbulent wall jet under adverse pressure gradient. It was found that the pressure distribution is hydrostatic only in a narrow region near the bed, and that the velocity distribution in the boundary layer part of the jump follows closely the velocity defect law for two-dimensional channel flow. Moreover, his experimental results showed a more accurate form of the momentum equation:

$$\left(\frac{d_2}{d_1}\right)^3 - \frac{d_2}{d_1}(1 - \varepsilon + 2F_1^2) + 2F_1^2 = 0 \quad (4)$$

where F_1 is the inflow Froude number, and ε is the dimensionless integrated shear force introduced by the author.

The dimensionless integrated shear force ε , introduced by Rajaratnam [7], was defined as:

$$\varepsilon = \frac{F_\tau}{0.5\gamma b_1 d_1^2} \quad (5)$$

where F_τ is the integrated bed shear stress over the hydraulic jump length; γ is the specific weight of water, and b_1 is the width of the stilling basin in upstream.

Later, McCorquodale and Khalifa [23] and Hager [15], studied the internal flow in hydraulic jumps and in particular the velocity distribution within the roller region.

Considering the studies of Resch et al., [24,25], Resch and Leutheusser [26], Roshko [27], Babb and Aus [28] and Hoyt and Sellin [29], it is believed that the flow of a jump must be analyzed in its actual configuration of air–water mixture, an aspect that cannot be overlooked. Ehrenberger [24] was the first to study the phenomenon of air entrainment in open channels. Resch and Leutheusser [25] were the first to show that the air entrainment

process, the transfer of momentum and energy dissipation are strongly affected by the inflow conditions. Using hot-film anemometry, Resch et al. [26] studied the distributions of air concentration and air-bubble dimensions in a hydraulic jump. The results of [26] suggested that a hydraulic jump with both undeveloped and fully developed inflows is similar to an aerator.

Roshko [27] observed that all shear flows are characterized by identifiable eddy structures, which are also present in a hydraulic jump and are responsible for the entrainment phenomenon, in agreement with [26]. Hoyt and Sellin [29] described a hydraulic jump using a mixing or shear layer model; in their investigation, the authors highlighted that the air entrainment phenomenon at the water surface of the analyzed hydraulic jump is a predominant feature and that a hydraulic jump is composed of coherent structures at the interface between air and water, with a density ratio of about 800.

2.2. Experimental Studies on the Turbulent Features of Hydraulic Jumps

However, the complex nature of the hydraulic jump, involving intense turbulence, velocity and pressure fluctuations and significant air entrainment, still showed that current knowledge is far from a full understanding of the phenomenon.

Most detailed air–water flow turbulent features of hydraulic jumps started to be systematically reported following [30]. However, few of the studies [30–33] reported air–water flow measurements accurately. The experiments of [30–33] specifically looked at the air–water properties in partially developed hydraulic jumps, and their results showed a likeness to plunging jet entrainment.

Mossa and Tolve [34] visualized the turbulent coherent structures in a hydraulic jump and determined the location of the maximum air concentration. Their results showed the existence of two regions with the greatest air concentration when the largest vortex of a hydraulic jump breaks down, causing the water to spill. Other results of their image analysis showed the presence of one region with a great air concentration when two neighboring vortices merged into a larger one.

Gualtieri and Chanson [35,36] studied the effect of the Froude number on the basic air–water flow properties, focusing on the maximum void fraction and bubble count rate in the shear layer. The air–water flow properties of a hydraulic jump were described in terms of the time-averaged void fraction, defined as the proportion of time that the probe tip is in the air, and the bubble count rate, defined as the number of bubbles impacting the probe tip per second. The void fraction and bubble count rate distributions in a vertical cross-section of jump rollers were measured in the literature with intrusive phase-detection techniques [32,34–44].

2.3. Experimental Studies on Oscillating Phenomena of Hydraulic Jumps

Some experimental studies highlighted the existence of oscillating phenomena and particularly, a cyclic variation of jump types over long-lasting experiments, under specific flow conditions [45–52]. Figure 4 summarizes the well-acknowledged flow patterns: (a) the A-jump, (b) the wave jump or W-jump, (c) the wave train, (d) the B-jump (or maximum plunging condition) characterized by a plunging jet mechanisms, and (e) the minimum B-jump (or limited jump) with a limited hydraulic jump.

Furthermore, Figure 4 shows pictures of flow conditions during experiments by Mossa et al. [50].

Experiments by [47] on local scour due to hydraulic jump formed on a sand bed showed that, for some runs, the hydraulic jump tended to repeat itself in a periodic form, from clockwise to anti-clockwise rotation of the vortex. Mossa [49,50] analyzed the oscillating characteristics typical of a hydraulic jump with an abrupt drop.

Flow conditions

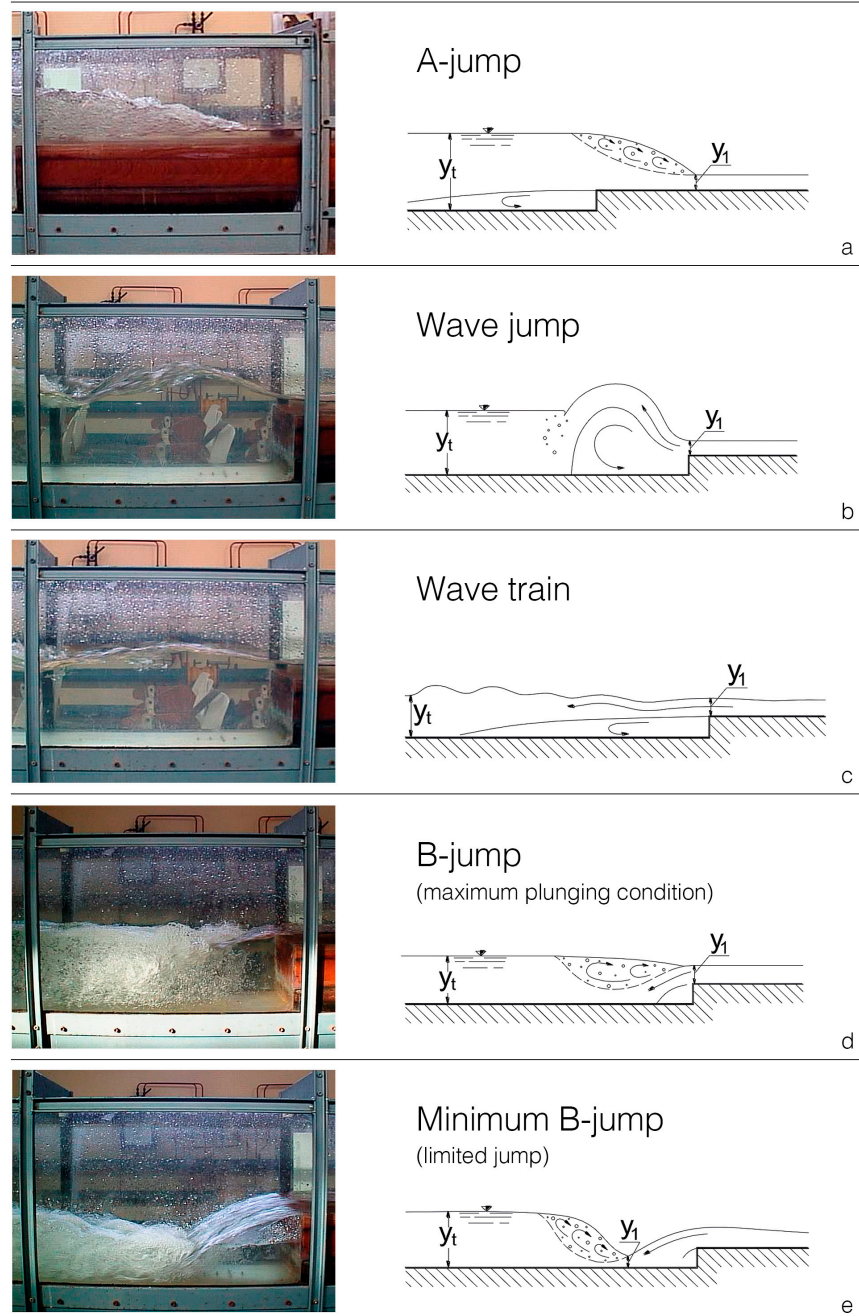


Figure 4. Flow conditions during experiments by Mossa et al. [50]. From the top: (a) A-jump; (b) wave jump; (c) wave train; (d) B-jump (maximum plunging condition); (e) minimum B-jump (limited jump).

Experiments in [49] were carried out in a channel with a non-erodible bottom (Figure 5), presenting a molded bed profile to investigate the oscillating characteristics of hydraulic jumps [47].

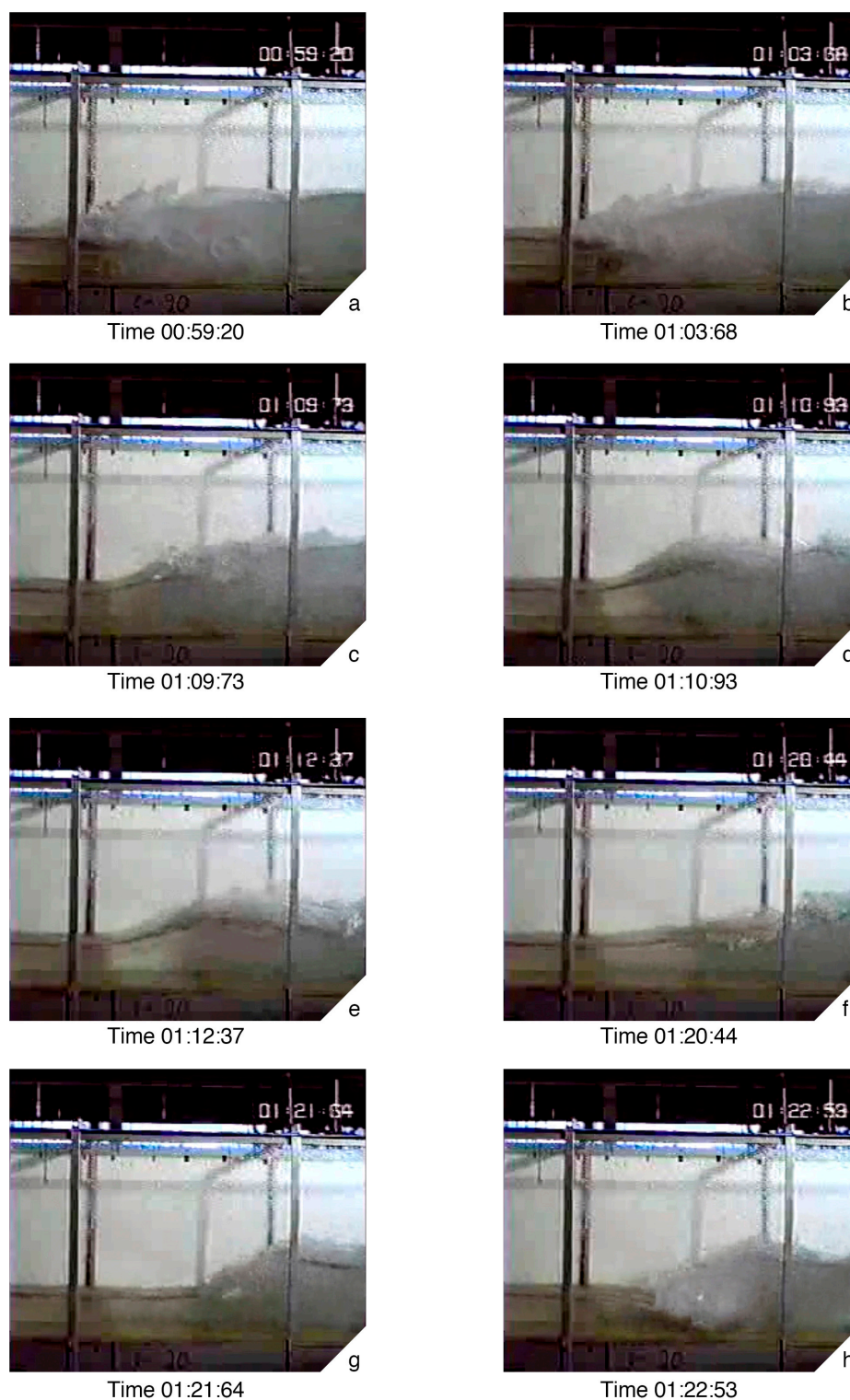


Figure 5. Oscillatory flow patterns between B-jumps and wave jumps (configuration B61 in Mossa et al. [50]); time is expressed in minutes, seconds, and hundredths of seconds from the start of filming (by Mossa et al. [50]): (a,b,g,h) B-jumps; (c–f) wave jumps. (See Video S2 in Supplementary Material).

This study showed how it is important to design basins considering the cyclic variation of jump types caused by the upstream and downstream flow conditions. The conclusions of the experiments in [49] may be summarized as follows:

oscillations of hydraulic jump types do not depend on whether the bottom is made of erodible or non-erodible material;
 a suitable time scale may be defined both for oscillations of the jump types and for fluctuations of the jump toes with a flat and outlined bottom;
 analysis of the oscillating phenomena indicates a correlation among the surface profile elevations, velocity components and pressure fluctuations;
 analysis of the oscillating phenomena indicates change configurations of the surface profile of a hydraulic jump, as a function of the air concentration present in the roller.

Successively, the experiments by Mossa et al. [50] considered the previous studies [47–49] in order to critically assess the basic flow patterns for the transition from super- to subcritical flows at an abrupt drop (Figure 5) and to propose new compelling conclusions pertaining to the changes of the different types of hydraulic jumps and the variation from one type to another. Figure 5 shows the oscillatory flow patterns between B-jumps (Figure 5a,b,g,h) and wave jumps (Figure 5c–f) (configuration B61 in Mossa et al. [50], where time is expressed in minutes, seconds and hundredths of seconds). Further details about the experimental tests can be found in [50].

The experimental observations [50] suggested designing basins and abrupt drops in order to take into consideration of different flow types, with the precautionary conditions as regards to the tail-water and pressure fluctuations in the channel.

In fact, experiments by [50] suggested that the relationship between the tail-water depth ratio and the upstream Froude number is a function of the relative step height. Furthermore, the experimental investigations by [50] also highlighted that the pressure fluctuations are quasi-periodic and heavily influenced by the oscillations between the B and wave jump types.

On this basis, more recently, experimental research was conducted by [53] focused on the fluctuating characteristics of the free surface and by [54,55] focused on the influence of velocity and pressure fluctuations on the hydraulic jump.

3. Research Challenges

Since the fluid dynamics problems are usually too complex to be solved by analytical methods because they involve many different issues due to their nonlinearity, research has recently focused on computer power and the continuous improvement of numerical codes. In recent years, the computational fluid dynamics (CFD) method, through turbulence models, has become a useful tool to study complex environmental fluid-mechanics problems. The numerical modeling of a hydraulic jump, which involves fluctuating boundaries as well as a multiphase flow, is still challenging, considering its complexity. Furthermore, whereas most of the experiments provide measurements at a point or on a plane, the complete three-dimensional (3D) flow field supplied by a CFD simulation would enable us to have a deeper understanding of the dynamics of coherent structures that are responsible for free-surface fluctuations and aeration in hydraulic jumps.

In recent years, hydraulic jumps have been investigated using both Eulerian and Lagrangian techniques. In general, the Eulerian method discretizes the space into a mesh and defines the unknown values at the fixed points, while the Lagrangian method tracks the pathway of each moving mass point. A comprehensive review of the studies, referring to the numerical simulation of the hydraulic jump was provided by Valero et al. [56] and Viti et al. [57].

3.1. Numerical Methods with an Eulerian Approach

Early Eulerian numerical studies on hydraulic jumps were carried out by Longo et al. [58], Chippada et al. [59], Qingchao and Drewes [60] and Cheng et al. [61].

Long et al. [58] simulated a submerged hydraulic jump with Froude numbers in the range of 3.2 to 8.2 on a smooth riverbed under the steady flow condition using a standard two-dimensional k-epsilon turbulence model.

In Chippada et al. [59], a detailed study of the internal and external characteristics of hydraulic jumps on a straight horizontal channel with supercritical Froude numbers 2 and 4 was numerically carried out by solving the RANS equations and a two-equation turbulence model. The results highlighted that surface rollers and recirculation zones play a dominant role in turbulence generation and dissipation.

In Qingchao and Drewes [60], the turbulent structures in the hydraulic jumps with Froude numbers in the range of 2.1 to 7.6 were investigated by means of the k-epsilon turbulent model.

Cheng et al. [61] introduced the volume of fluid (VOF) model to trace the free water surface and simulate the hydraulic jumps on a corrugated riverbed under five different conditions.

However, these simulations of hydraulic jumps were confined to the liquid phase and ignored the effect of the entrained air; early numerical studies that considered the air entrainment in the hydraulic jump were carried out by Souders and Hirt [62] and by Gonzalez and Bombardelli [63]. However, both of these studies provide only qualitative predictions of two-phase fluid field properties without quantitative comparisons with experimental ones.

Therefore, the first numerical results to be compared with experimental void fraction data were supplied by Ma et al. [64], using both RANS (Reynolds-averaged Navier–Stokes) and DES (detached eddy simulation)-type turbulence models

More recently, Witt et al. [65] used a volume of fluid (VOF) model for free-surface tracking in conjunction with a RANS model to study air entrainment in a hydraulic jump.

Recently, Bayon et al. [66] studied the air entrainment in a steady hydraulic jump of a Froude number 6.5 using a RNG- k-epsilon turbulent model and the volume of fluid (VOF) model. Wei et al. [67] reported numerical results showing that the energy dissipation rate correlated with the Froude number.

3.2. Numerical Methods with a Lagrangian Approach

Although less widely researched, the Lagrangian meshless method showed interesting results; in fact, meshless Lagrangian techniques appear, in general, to be more suitable for capturing the highly unsteady free surface of a hydraulic jump. Smoothed particle hydrodynamics (SPH), which is one of the most popular mesh-free methods, was introduced by [68,69]. In the SPH technique, materials with different physical properties are discretized by convenient particle sets, each characterized by specific physical properties and constitutive laws. This feature allows for the modeling of multi-phase flows [70]. Refer to [71,72] textbooks and review articles for a general description of SPH.

In SPH simulations by Lopez et al. [73], a mobile hydraulic jump for different Froude numbers was investigated. Numerical simulations were compared to their own physical model. The results showed a good agreement for Froude numbers <5 with a Monaghan artificial viscosity. However, for higher Froude numbers, a k-epsilon turbulent model was required.

In SPH simulations by Federico et al. [74], by varying the Froude number, several types of jumps were investigated with specific focus on the velocity field, pressure forces, water depths and the location of the jump. Results showed good agreement with theory and experimental data.

In Jonsson et al. [75], the hydraulic jump was investigated with smoothed particle hydrodynamics, applying a new approach for periodic open boundary conditions. The jump toe oscillated with a frequency in good agreement with experimental findings found in the literature, and the oscillation amplitude increased with Froude number.

In Chern and Syamsuri [76] and Gu et al. [77], a smoothed particle hydrodynamics (SPH) model was applied to investigate the effect of various corrugated beds on the hydraulic jump.

In De Padova et al. [78], the formation of undular hydraulic jumps for different Froude numbers in a very large channel was investigated using a weakly compressible smoothed

particle (WCSPH) scheme with both an algebraic mixing-length model and a two-equation turbulence model.

Until the end of the 90s, in spite of the many experimental studies on the hydraulic jump, the complex structure of the separated region in very large channels downstream of the lateral shockwaves was not yet understood [79]. Consequently, experimental research was conducted by Ben Meftah et al. [80–82] on hydraulic jumps in a very large channel.

The numerical results [82] showed that the predictions gained by using the SPH model are in good agreement with experimental ones [80–82] in terms of the time-averaged water depth (Figure 6b) and longitudinal velocity components (Figure 6c), as well as the trapezoidal wave pattern and the size and magnitude of the recirculation regions along the lateral walls (Figure 6a–d). In particular, Figure 6c shows both SPH (black) and experimental (red) velocity fields superimposed in a vector plot. As experimentally observed, it can be seen that the wall boundary layer is subjected to a sudden adverse pressure gradient, causing a sharp deceleration of the flow velocity near the wall; furthermore, recirculation of the flow immediately behind the lateral shockwaves near the wall is observed. Further details about the numerical tests can be found in [79].

In De Padova et al. [83,84], a weakly compressible smoothed particle (WCSPH) model was applied to the modeling of a hydraulic jump at an abrupt drop. The complete spatial and temporal knowledge of the flow yielded by the SPH simulations improved the understanding of the phenomena without resorting to additional extensive experimental activity.

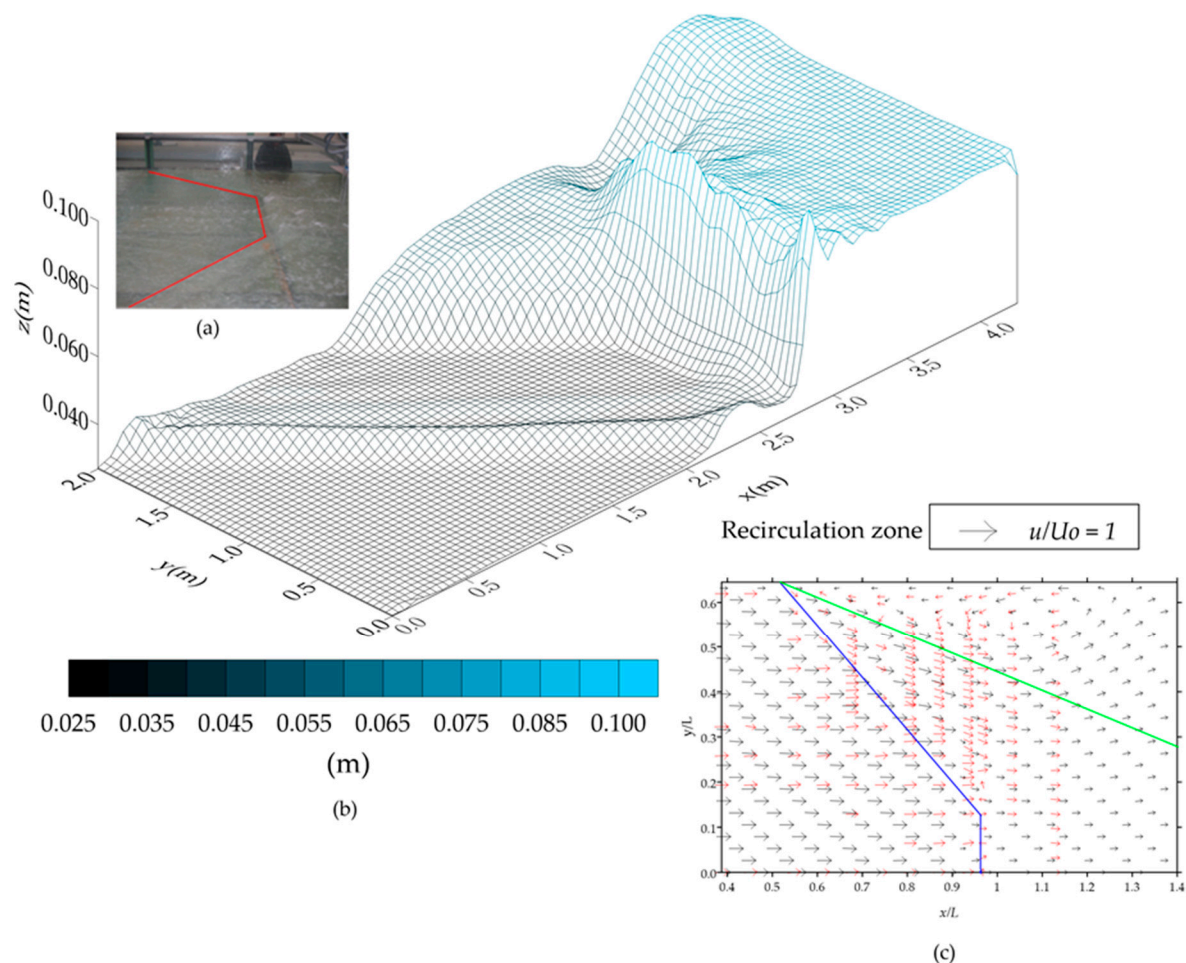


Figure 6. SPH simulation of hydraulic jump in a very large channel: (a) picture of experiment; (b) wave-height distribution and (c) velocity vector fields.

A comparison with experimental results by [50] showed that the SPH simulations were able to reproduce the main characteristics of this phenomenon, which, under the inflow and tail-water flow conditions, can lead to cyclic oscillations between jump types and jump vortices.

As shown in Figure 7, the simulated oscillatory flow patterns between A jumps and wave jumps reproduce what was observed in configuration B39 in Mossa et al. [50].

Vortices are characterized by a clockwise rotation (positive vorticity) when the wave jump occurs (Figure 7b,c) and by an anti-clockwise one (negative vorticity) for the A jump (Figure 7a,d), respectively. These numerical results highlight that a strong correlation exists among the velocity and vorticity fields and the pressure fluctuations, even far downstream of the jump position.

Further details about the numerical tests can be found in [83,84].

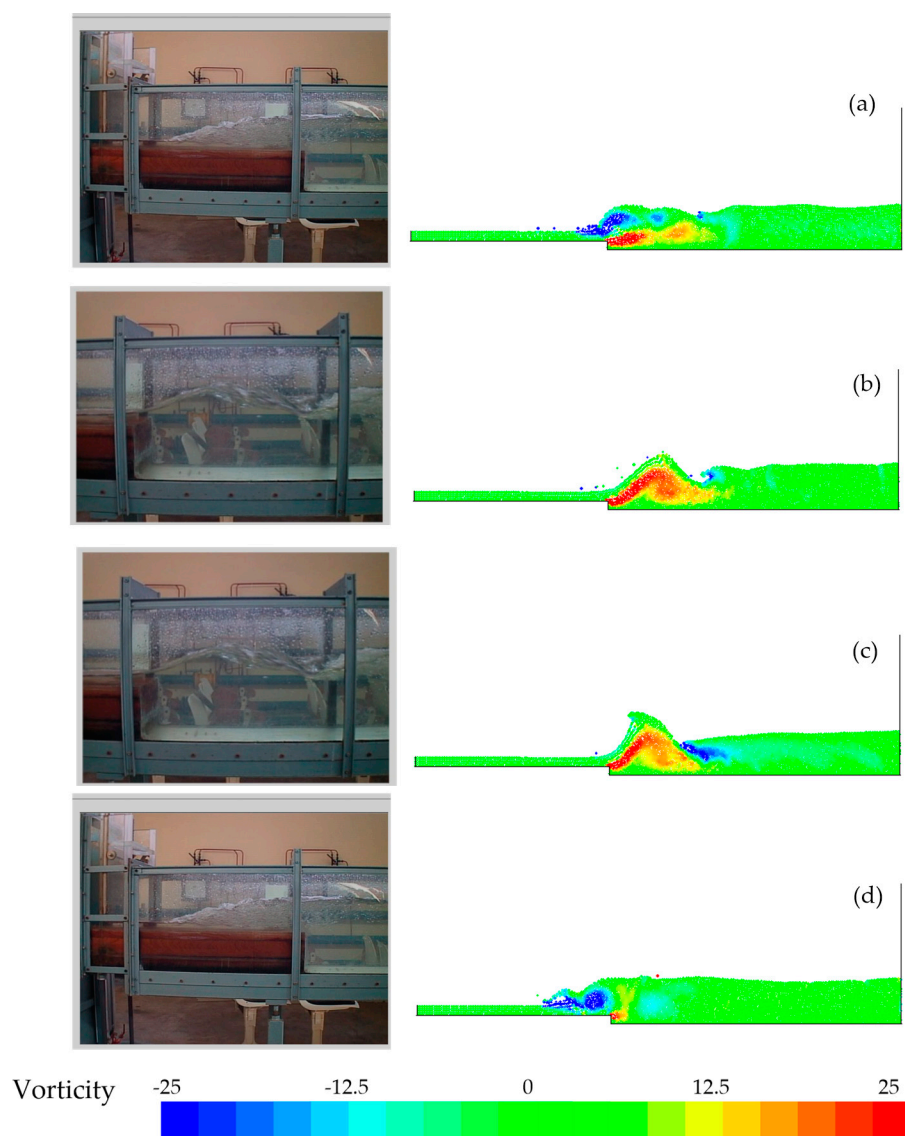


Figure 7. SPH vorticity field; oscillatory flow patterns between A-jumps and wave jumps: (a) $t = 2$ s; (b) $t = 4$ s; (c) $t = 8.5$ s and (d) $t = 11.5$ s.

4. Conclusions

The complicated nature of the hydraulic jump has always attracted researchers' attention. After many years of sustained research and with many of its features now well

understood, a satisfactory and full comprehension of this complex phenomenon remains a challenge.

Leonardo da Vinci first noticed this phenomenon, but it was only later in 1820 that Bidone started to study it scientifically. Since the beginning of the 20th century, the hydraulic jump has received a lot of attention, following the development of energy dissipater designs and stilling basins.

Several experimental studies in the late 1920s and early 1930s investigated the surface roller profile and energy dissipation. Then, in the late 1950s, the study of internal flow features started, and experimental research activity focused on turbulence estimations in hydraulic jumps.

In the 70s, it was believed that the flow of a jump must be analyzed in its actual configuration of air–water mixture, an aspect that cannot be overlooked. Therefore, several experimental studies were conducted to visualize the turbulent coherent structures in a hydraulic jump and to determine the location of the maximum air concentration.

The experimental results showed the existence of two regions with the greatest air concentration when the largest vortex of a hydraulic jump breaks down, causing the water to spill.

More recently, the effect of the Froude number on the basic air–water flow properties, focusing on the maximum void fraction and bubble count rate in the shear layer, was studied.

Several experimental studies in the late 1980s and 1990s highlighted the existence of oscillating phenomena and particularly, a cyclic variation of jump types over long-lasting experiments, under specific flow conditions, and investigated the surface roller profile and energy dissipation. Experimental observations led to the conclusion that the oscillating phenomena were especially significant for the analysis of turbulence characteristics.

Until the end of the 90s, in spite of the many experimental studies on hydraulic jump, the complex structure of the separated region in very large channels downstream of the lateral shockwaves was not yet understood. The first experimental research on hydraulic jumps in a very large channel suggested that the wall boundary layer is subjected to a sudden adverse pressure gradient, causing a sharp deceleration of the flow velocity near the wall; moreover, the experiments showed a recirculation of the flow immediately behind the lateral shockwaves near the wall.

While most of the experiments provide measurements at a point or on a plane, the complete three-dimensional (3D) flow field supplied by a CFD simulation enables us to have a deeper understanding of the dynamics of coherent structures that are responsible for free-surface fluctuations and aeration in hydraulic jumps.

Therefore, in recent years, the computational fluid dynamics (CFD) method, through turbulence models, has become a useful tool to study complex environmental fluid-mechanics problems.

The numerical modeling of a hydraulic jump, which involves fluctuating boundaries, as well as a multiphase flow, is still challenging, considering its complexity. Hydraulic jumps have been widely investigated using Eulerian techniques showing satisfactory results in terms of quantity and quality; Eulerian models, by solving the RANS equations, and a two-equation turbulence model have yielded accurate results for mean flow variables, including air concentrations in some cases.

In the last few decades, although less researched, the Lagrangian meshless method showed interesting results; in fact, meshless Lagrangian techniques appear in general to be more suitable for capturing the highly unsteady free surface of a hydraulic jump.

Nevertheless, it is evident that the profitable prediction of a numerical model depends on the calibration made with experimental data.

Therefore, the mean flow variables (sequent depths' relationship, roller length, jump length, mean free surface profile, air concentrations, etc.) that have been extensively experimentally studied in the literature should constitute the minimum dataset for numerical models' calibration.

Supplementary Materials: The following are available online at <http://doi.org/10.5281/zenodo.4423177>, Video S1: Oscillations-jump.mp4. The video shows the oscillatory flow patterns between B-jump and Wave jump (Figure 5), Video S2: Und-jump_large_channel.mp4. The video shows a hydraulic jump in the large channel of the LIC—Coastal Engineering Laboratory of the Polytechnic University of Bari, Italy (Figure 1).

Author Contributions: M.M. conceived and designed the experiments; M.M. performed the experiments; M.M. and D.D.P. contributed analysis tools; M.M. and D.D.P. wrote the paper. All authors have read and agreed to the published version of the manuscript.

Funding: This research received no external funding.

Institutional Review Board Statement: Not applicable.

Informed Consent Statement: Not applicable.

Data Availability Statement: Data available presented in this study are openly available in Zenodo at <http://doi.org/10.5281/zenodo.4423177> (accessed on 7 January 2021).

Conflicts of Interest: The authors declare no conflict of interest.

References

1. Bidone, G. Expériences sur la propagation des remous. In *Memorie Della Reale Accademia delle Scienze di Torino*; Natural History Museum Library: London, UK, 1820; Volume 30, pp. 195–292.
2. Guglielmini, D. *Della Natura de' Fiumi*; Nuova Edizione con le Annotazioni di Eustachio Manfredi: Bologna, Italy, 1739.
3. Bélanger, J.B. *Essai sur la Solution Numérique de Quelques Problèmes Relatifs au Mouvement Permanent des Eaux Courantes* ('*Essay on the Numerical Solution of Some Problems relative to Steady Flow of Water*'); Carilian-Goeury: Paris, France, 1828.
4. Leutheusser, H.J.; Alemu, S. Flow separation under hydraulic jump. *J. Hydraul. Res.* **1978**, *17*, 193–206. [\[CrossRef\]](#)
5. Harleman, D.R.F. Discussion of "Turbulence characteristics of the hydraulic jump" by Rouse, H., Siao, T. T., & Nagaratnam, S. *Trans. ASCE* **1959**, *124*, 959–962.
6. Peterka, A.J. *Hydraulic Design of Stilling Basins and Energy Dissipators*; United States Department of the Interior: Washington, DC, USA, 1958.
7. Rajaratnam, N. The Hydraulic Jump as a Wall Jet. *J. Hydraul. Div.* **1965**, *91*, 107–132. [\[CrossRef\]](#)
8. Leutheusser, H.J.; Kartha, V.C. Effects of inflow conditions on hydraulic jump. *J. Hydraul. Div.* **1972**, *98*, 1367–1385. [\[CrossRef\]](#)
9. Hager, W.H.; Bretz, N.V. Hydraulic jumps at positive and negative steps. *J. Hydraul. Res.* **1986**, *24*, 237–252. [\[CrossRef\]](#)
10. Hager, W.H.; Bremen, R. Classical hydraulic jump: Sequent depths. *J. Hydraul. Res.* **1989**, *27*, 565–585. [\[CrossRef\]](#)
11. Hager, W.H. *History of the Hydraulic Jump, United States*; Bureau of Reclamation, U.S. Department of the Interior, Bureau of Reclamation, Engineering and Research Center: Washington, DC, USA, 1990.
12. Wu, S.; Rajaratnam, N. Free jumps, submerged jumps and wall jets. *J. Hydraul. Res.* **1995**, *33*, 197–212. [\[CrossRef\]](#)
13. Carollo, F.G.; Ferro, V.; Pampalone, V. New solution of classical hydraulic jump. *J. Hydraul. Eng.* **2009**, *135*, 527–531. [\[CrossRef\]](#)
14. Vischer, D.L.; Hager, W.H. *Dam Hydraulics*; John Wiley Sons: Chichester, UK, 1998.
15. Hager, W.H. *Energy Dissipators and Hydraulic Jump*; Water Science and Technology Library; Springer Science & Business Media: Dordrecht, The Netherlands, 1992; Volume 8, ISBN 978-90-481-4106-7.
16. Riegel, R.M.; Beebe, J.C. *The Hydraulic Jump as a Means of Dissipating Energy*; Technical Reports Part III; Miami Conservancy District: Dayton, OH, USA, 1917; pp. 60–111.
17. Rehbock, T. Die Bekämpfung der Sohlen-Auskolkung bei Wehren durch Zahnschwellen. *Schweiz. Bauzt.* **1926**, *87*, 27–31.
18. Safranez, K. Wechselsprung und die Energievernichtung des Wassers. *Bauingenieur* **1927**, *8*, 898–905. (In German).
19. Bakhmeteff, B.A. *Hydraulics of Open Channels*, 1st ed.; McGraw-Hill: New York, NY, USA, 1932.
20. Rouse, H. On the Use of Dimensionless Numbers. *Civil Eng.* **1934**, *4*, 563–568.
21. Bakhmeteff, B.A.; Matzke, A.E. The hydraulic jump in terms of dynamic similarity. *ASCE Trans.* **1936**, *101*, 630–680.
22. Rouse, H.; Siao, T.T.; Nagaratnam, S. Turbulence characteristics of the hydraulic jump. *J. Hydraul. Div.* **1958**, *84*, 1–30.
23. McCorquodale, J.A.; Khalifa, A. Internal flow in hydraulic jumps. *J. Hydraul. Eng.* **1983**, *109*, 684–701. [\[CrossRef\]](#)
24. Ehrenberger, I. Wasserbewegung in Steilen Rinnen (Susstennen). mit Besonderer Berücksichtigung der Selbstbelüftung. *Z. Osterr. Ing. Archit.* **1926**. No. 15/16 and 17/18 (In German).
25. Resch, F.J.; Leutheusser, H.J. Le ressaut hydraulique: Measure de turbulence dans la region diphasique. (The hydraulic jump: Turbulence measurements in the two-phase flow region). *J. Houille Blanche* **1972**, *4*, 279–293. (In French). [\[CrossRef\]](#)
26. Resch, F.J.; Leutheusser, H.J.; Alemu, S. Bubbly two-phase flow in the hydraulic jump. *J. Hydraul. Div.* **1974**, *84*, 137–149. [\[CrossRef\]](#)
27. Roshko, A. Structure of turbulent shear flows: A new look. *AIAA J.* **1976**, *14*, 1349–1357. [\[CrossRef\]](#)
28. Babb, A.F.; Aus, H.C. Measurements of Air in Flowing Water. *J. Hydraul. Div.* **1981**, *107*, 1615–1630. [\[CrossRef\]](#)
29. Hoyt, J.W.; Sellin, R.H.J. Hydraulic jump as "mixing layer". *J. Hydraul. Eng.* **1989**, *115*, 1607–1613. [\[CrossRef\]](#)

30. Chanson, H.; Qiao, G.L. *Air Bubble Entrainment and Gas Transfer at Hydraulic Jumps*; Research Report No. CE149; Department of Civil Engineering, University of Queensland: Brisbane, QLD, Australia, 1994; p. 68.
31. Chanson, H. *Air Bubble Entrainment in Free-Surface Turbulent Flows*; Experimental Investigations. Report CH46/95; Department of Civil Engineering, University of Queensland: Brisbane, QLD, Australia, 1995; p. 368.
32. Chanson, H. Air entrainment in two-dimensional turbulent shear flows with partially developed inflow conditions. *Int. J. Multiph. Flow* **1995**, *21*, 1107–1121. [[CrossRef](#)]
33. Chanson, H.; Brattberg, T. Experimental study of the air–water shear flow in a hydraulic jump. *Int. J. Multiph. Flow* **2000**, *26*, 583–607. [[CrossRef](#)]
34. Mossa, M.; Tolve, U. Flow visualization in bubbly two-phase hydraulic jump. *J. Fluids Eng.* **1998**, *120*, 160–165. [[CrossRef](#)]
35. Gualtieri, C.; Chanson, H. Experimental Analysis of Froude Number Effect on Air Entrainment in the Hydraulic Jump. *Environ. Fluid Mech.* **2007**, *7*, 217–238. [[CrossRef](#)]
36. Gualtieri, C.; Chanson, H. Effect of Froude number on bubble clustering in a hydraulic jump. *J. Hydraul. Res.* **2010**, *48*, 504–508. [[CrossRef](#)]
37. Gualtieri, C.; Chanson, H. Interparticle arrival time analysis of bubble distributions in a dropshaft and hydraulic jump. *J. Hydraul. Res.* **2013**, *51*, 253–264. [[CrossRef](#)]
38. Chanson, H. Hydraulic Jumps: Turbulence and Air Bubble Entrainment. *J. Houille Blanche* **2011**, *3*, 5–16. [[CrossRef](#)]
39. Kucukali, S.; Chanson, H. Turbulence Measurements in Hydraulic Jumps with Partially-Developed Inflow Conditions. *Exp. Therm. Fluid Sci.* **2008**, *33*, 41–53. [[CrossRef](#)]
40. Murzyn, F.; Chanson, H. Experimental Investigation of Bubbly Flow and Turbulence in Hydraulic Jumps. *Environ. Fluid Mech.* **2009**, *9*, 143159. [[CrossRef](#)]
41. Chachereau, Y.; Chanson, H. Bubbly flow measurements in hydraulic jumps with small inflow Froude numbers. *Int. J. Multiph. Flow* **2011**, *37*, 555–564. [[CrossRef](#)]
42. Wang, H. Turbulence and Air Entrainment in Hydraulic Jumps. Ph.D. Thesis, School of Civil Engineering, The University of Queensland, Brisbane, QLD, Australia, 2014. [[CrossRef](#)]
43. Felder, S.; Chanson, H. Turbulence, Dynamic Similarity and Scale Effects in High-Velocity Free-Surface Flows above a Stepped Chute. *Exp. Fluids* **2009**, *47*, 1–18. [[CrossRef](#)]
44. Long, D.; Rajaratnam, N.; Steffler, P.M.; Smy, P.R. Structure of flow in hydraulic jumps. *J. Hydraul. Res.* **1991**, *29*, 207–218. [[CrossRef](#)]
45. Ohtsu, I.; Yasuda, Y. Transition from supercritical to subcritical flow at an abrupt drop. *J. Hydraul. Res.* **1991**, *29*, 309–328. [[CrossRef](#)]
46. Habib, E.; Mossa, M.; Petrillo, A. Scour downstream of hydraulic jump. In Proceedings of the Modeling, Testing & Monitoring for Hydro Powerplants Conference, Budapest, Hungary, 11–13 July 1994; pp. 591–602.
47. Abdel Ghafar, A.; Mossa, M.; Petrillo, A. Scour from flow downstream of a sluice gate after a horizontal apron. In Proceedings of the 6th International Symposium on River Sedimentation, New Delhi, India, 7–11 November 1995; pp. 1069–1088.
48. Chanson, H.; Toombes, L. Supercritical flow at an abrupt drop: Flow patterns and aeration. *Can. J. Civil Eng.* **1998**, *25*, 956–966. [[CrossRef](#)]
49. Mossa, M. On the oscillating characteristics of hydraulic jumps. *J. Hydraul. Res.* **1999**, *37*, 541–558. [[CrossRef](#)]
50. Mossa, M.; Petrillo, A.; Chanson, H. Tailwater Level Effects on Flow Conditions at an Abrupt Drop. *J. Hydraul. Res.* **2003**, *41*, 39–51. [[CrossRef](#)]
51. Mok, K.M.; Mossa, M. Discussion on: Relation of surface roller eddy formation and surface fluctuation in hydraulic jumps. *J. Hydraul. Res.* **2004**, *42*, 207–212. [[CrossRef](#)]
52. Mossa, M.; Petrillo, A.; Chanson, H.; Yausda, Y.; Takahashi, M.; Ohtsu, I. Discussion on Tailwater level effects on flow conditions at an abrupt drop. *J. Hydraul. Res.* **2005**, *43*, 217–224. [[CrossRef](#)]
53. Wang, H.; Chanson, H. Experimental study of turbulent fluctuations in hydraulic jumps. *J. Hydraul. Eng.* **2015**, *141*, 04015010. [[CrossRef](#)]
54. Chachereau, Y.; Chanson, H. Free-surface fluctuations and turbulence in hydraulic jumps. *Exp. Therm. Fluid Sci.* **2011**, *35*, 896–909. [[CrossRef](#)]
55. Zhang, G.; Wang, H.; Chanson, H. Turbulence and aeration in hydraulic jumps: Free-surface fluctuation and integral turbulent scale measurements. *Environ. Fluid Mech.* **2013**, *13*, 189–204. [[CrossRef](#)]
56. Valero, D.; Viti, N.; Gualtieri, C. Numerical Simulation of Hydraulic Jumps. Part 1: Experimental Data for Modelling Performance Assessment. *Water* **2018**, *11*, 36. [[CrossRef](#)]
57. Viti, N.; Valero, D.; Gualtieri, C. Numerical Simulation of Hydraulic Jumps. Part 2: Recent Results and Future Outlook. *Water* **2019**, *11*, 28. [[CrossRef](#)]
58. Long, D.; Steffler, P.M.; Rajaratnam, N. A numerical study of submerged hydraulic jumps. *J. Hydraul. Res.* **1991**, *29*, 293–308. [[CrossRef](#)]
59. Chippada, S.; Ramaswamy, B.; Wheeler, M.F. Numerical simulation of hydraulic jump. *Int. J. Numer. Methods Eng.* **1994**, *37*, 1381–1397. [[CrossRef](#)]
60. Qingchao, L.; Drewes, U. Turbulence characteristics in free and forced hydraulic jumps. *J. Hydraul. Res.* **1994**, *32*, 877–898. [[CrossRef](#)]

61. Cheng, X.; Chen, Y. Numerical simulation of hydraulic jumps on corrugated beds. *J. Hydraul. Eng.* **2005**, *10*, 52–57.
62. Souders, D.T.; Hirt, C.W. Modeling entrainment of air at turbulent free surfaces. In Proceedings of the World Water and Environmental Resources Congress 2004, Salt Lake City, UT, USA, 27 June–1 July 2004.
63. Gonzalez, A.E.; Bombardelli, F.A. Two-phase-flow theoretical and numerical models for hydraulic jumps, including air entrainment. In Proceedings of the XXXI IAHR Congress 2005, Seoul, Korea, 11–16 September 2005.
64. Ma, J.; Oberai, A.A.; Lahey, R.T., Jr.; Drew, D.A. Modeling air entrainment and transport in a hydraulic jump using two-fluid RANS and DES turbulence models. *Heat Mass Transf.* **2011**, *47*, 911–919. [[CrossRef](#)]
65. Witt, A.; Gulliver, J.; Shen, L. Simulating air entrainment and vortex dynamics in a hydraulic jump. *Int. J. Multiph. Flow* **2015**, *72*, 165–180. [[CrossRef](#)]
66. Bayon, A.; Valero, D.; García-Bartual, R.; Vallés-Morán, F.J.; López-Jiménez, P.A. Performance assessment of OpenFOAM and FLOW-3D in the numerical modeling of a low Reynolds number hydraulic jump. *Environ. Model. Softw.* **2016**, *80*, 322–335. [[CrossRef](#)]
67. Wei, W.; Hong, Y.; Liu, Y. Numerical Simulation on Hydraulic Characteristics of Free Hydraulic Jump on Corrugated Beds of Stilling Basin. *J. Syst. Simul.* **2017**, *29*, 918–925.
68. Gingold, R.A.; Monaghan, J.J. Smoothed particle hydrodynamics: Theory and application to nonspherical stars. *Monthly Not. R. Astron. Soc.* **1977**, *181*, 375–389. [[CrossRef](#)]
69. Lucy, L. A numerical approach to the testing of fusion process. *Astronom. J.* **1977**, *82*, 1013–1024. [[CrossRef](#)]
70. De Padova, D.; Mossa, M. Multi-phase simulation of infected respiratory cloud transmission in air. *AIP Adv.* **2021**, *11*. [[CrossRef](#)]
71. Gomez-Gesteira, M.; Rogers, B.D.; Darlymple, R.A.; Crespo, A.J.C. State-of-the-art of classical SPH for free-surface flows. *J. Hydraul. Res.* **2010**, *48*, 6–27. [[CrossRef](#)]
72. De Padova, D.; Meftah, M.B.; De Serio, F.; Mossa, M.; Sibilla, S. Characteristics of breaking vorticity in spilling and plunging waves. *Environ. Fluid Mech.* **2020**, *20*, 233–260. [[CrossRef](#)]
73. López, D.; Marivela, R.; Garrote, L. Smoothed particle hydrodynamics model applied to hydraulic structures: A hydraulic jump test case. *J. Hydraul. Res.* **2010**, *48*, 142–158. [[CrossRef](#)]
74. Federico, I.; Marrone, S.; Colagrossi, A.; Aristodemo, F.; Antuono, M. Simulating 2D open channel flows through an SPH model. *Eur. J. Mech. B/Fluids* **2012**, *34*, 35–46. [[CrossRef](#)]
75. Jonsson, P.; Andreasson, P.; Gunnar, J.; Hellström, I.; Jonsén, P.; Staffan Lundström, T. Smoothed Particle Hydrodynamic simulation of hydraulic jump using periodic open boundaries. *Appl. Math. Model.* **2016**, *40*, 8391–8405. [[CrossRef](#)]
76. Chern, M.J.; Syamsuri, S. Effect of corrugated bed on hydraulic jump characteristic using SPH method. *J. Hydraul. Eng.* **2012**, *139*, 221–232. [[CrossRef](#)]
77. Gu, S.; Bo, F.; Luo, M.; Kazemi, E.; Zhang, Y.; Wei, J. SPH Simulation of Hydraulic Jump on Corrugated Riverbeds. *Appl. Sci.* **2019**, *9*, 436. [[CrossRef](#)]
78. De Padova, D.; Mossa, M.; Sibilla, S.; Torti, E. 3D SPH modeling of hydraulic jump in a very large channel. *J. Hydraul. Res.* **2010**, *51*, 158–173. [[CrossRef](#)]
79. Chanson, H.; Montes, J.S. Characteristics of undular hydraulic jump: Experimental apparatus and flow patterns. *J. Hydraul. Eng.* **1995**, *121*, 129–144. [[CrossRef](#)]
80. Meftah, M.B.; De Serio, F.; Mossa, M.; Pollio, A. Analysis of the velocity field in a large rectangular channel with lateral shockwave. *Environ. Fluid Mech.* **2007**, *7*, 519–536. [[CrossRef](#)]
81. Meftah, M.B.; De Serio, F.; Mossa, M.; Pollio, A. Experimental study of recirculating flows generated by lateral shock waves in very large channels. *Environ. Fluid Mech.* **2008**, *8*, 215–238. [[CrossRef](#)]
82. Meftah, M.B.; Mossa, M.; Pollio, A. Considerations on shock wave/boundary layer interaction in undular hydraulic jumps in horizontal channels with a very high aspect ratio. *Eur. J. Mech. B Fluids* **2010**, *29*, 415–429. [[CrossRef](#)]
83. De Padova, D.; Mossa, M.; Sibilla, S. SPH modelling of hydraulic jump oscillations at an abrupt drop. *Water* **2017**, *9*, 790. [[CrossRef](#)]
84. De Padova, D.; Mossa, M.; Sibilla, S. SPH numerical investigation of the characteristics of an oscillating hydraulic jump at an abrupt drop. *J. Hydrodyn.* **2018**, *30*, 106–113. [[CrossRef](#)]